Available online at www.sciencedirect.com
SCIENCE DIRECT
ELSEVIER
International Journal of Mechanical Sciences 48 (2006) 53–61
International Journal of MECHANICAL SCIENCES
www.elsevier.com/locate/ijmecsci

Investigation of buckling of double-walled carbon nanotubes embedded in an elastic medium using the energy method

Y.Q. Zhang[a,*], G.R. Liu[b], H.F. Qiang[c], G.Y. Li[d]

[a]*School of Civil and Environmental Engineering, Nanyang Technological University, Nanyang Avenue, Singapore 639798, Singapore*
[b]*Centre for Advanced Computations in Engineering Science, Department of Mechanical Engineering, National University of Singapore, 10 Kent Ridge Crescent, Singapore 119260, Singapore*
[c]*Xi'an Hi-Tech Institute, Xi'an 710025, China*
[d]*Department of Mechanical Engineering, Hunan University, Changsha 410082, China*

Received 3 June 2004; received in revised form 14 August 2005; accepted 17 September 2005
Available online 25 October 2005

Abstract

Elastic buckling of a long double-walled carbon nanotube embedded in an elastic medium and subjected to a far-field hydrostatic pressure is analyzed using the energy method. The study is on the basis of elastic-shell models at nano-scale, and the effect of van der Waals forces on the buckling is considered. The double-walled carbon nanotube is assumed to be thin and the tube is taken to be perfectly bonded to the surrounding medium. Both normal and shear stresses at the outer tube-medium interface are included. The difference between the Poisson's ratio of the tube and that of the elastic medium is taken into account. An expression is derived relating the external pressure to the buckling mode number, from which the critical pressure can be obtained. As a result, the critical pressure is dependent on the inner radius-to-thickness ratio, the material parameters of the elastic medium, and the van der Waals force.

Keywords: Elastic buckling; Carbon nanotubes; Elastic medium; Energy method

1. Introduction

Since their first discovery and the establishment of new effective methods for production, carbon nanotubes (CNTs) have drawn a great deal of attention and a good many stimulated extensive studies [1–10]. Both experimental and theoretical studies showed that CNTs have exceptional mechanical and electronic properties such as high stiffness-to-weight and strength-to-weight ratios and enormous electrical and thermal conductivities [11–13]. CNTs are cylindrical macromolecules composed of carbon atoms in a periodic hexagonal arrangement. The diameter of a CNT is generally between 0.7 and 10 nm, and the length can be as large as 10^4–10^5 times the diameter [14]. CNTs can be produced by an array of techniques, such as arc discharge, laser ablation and chemical vapor deposition. Depending on the synthesis conditions, nanotubules can be single-walled (a single tubule) or multi-walled (2–50 tubules positioned concentrically within one another). Due to their remarkable mechanical, physical and chemical properties, CNTs have emerged as potentially attractive materials as reinforcing elements in composite materials.

As most potential applications of CNTs are heavily based on a thorough understanding of their mechanical behavior [15,16], the study of mechanical behavior of CNTs has been one topic of major concern [11,17–20]. Besides the great deal of experimental works on CNTs, investigation of mechanical response of CNTs by theoretical modeling has been pursued [12,14]. These modeling approaches can be generally classified into two categories. One is the atomistic modeling and the other is the continuum mechanics modeling. The major techniques of the atomistic modeling include classical molecular dynamics (MD), tight-binding molecular dynamics (TBMD) and density functional theory (DFT). However, being very time consuming and computationally expensive for large-sized atomic systems, practical applications of these

*Corresponding author. Tel.: +65 679 06 199; fax: +65 679 106 76.
E-mail address: cyqzhang@ntu.edu.sg (Y.Q. Zhang).

0020-7403/$ - see front matter © 2005 Elsevier Ltd. All rights reserved.
doi:10.1016/j.ijmecsci.2005.09.010

atomistic modeling techniques are very limited. Consequently, it is desirable to develop continuum theories that may overcome the limitations of atomistic simulations concerning both time and length scales. Recently, continuum mechanics models have been widely and successfully used to study carbon nanotubes [11,18–22]. These prior studies indicated that "the laws of continuum mechanics are amazingly robust and allow one to treat even intrinsically discrete objects only a few atoms in diameter" [23]. Thus, continuum mechanics models will continue to play an important role in the study of CNTs as experiments at the nanoscale are extremely difficult and atomistic modeling remains prohibitively expensive for large-sized atomic systems.

When CNTs are subjected to external loads, the phenomenon of buckling is often observed owing to their large aspect ratio and tube-like geometry. Hence, buckling of CNTs has been the subject of numerous experimental, molecular-dynamics and theoretical simulations [11,21–26]. Yakobson et al. [11] compared the results of atomistic modeling for axially compressed buckling of single-walled nanotubes with a simple continuum shell model, and found that all changes of buckling patterns given by the molecular-dynamics simulations can be predicted satisfactorily by the continuum shell model. Ru [27] developed an elastic honeycomb model for single-walled carbon nanotube (SWNT) ropes and obtained a simple critical buckling pressure formula which gave a result in good agreement with known experimental data. On account of the strong evidence [17,28,29] that the van der Waals forces play an essential role in the interaction of CNTs, especially for the multi-walled carbon nanotubes (MWNTs), Ru [30] presented an elastic shell model to study infinitesimal buckling of a DWNT under axial compression including the effect of van der Waals forces. In addition, considerable effort has been devoted to MWNTs embedded in a polymer or metal matrix [22,31,32], where hydrostatic compressive stress due to thermal mismatch and specimen cooling is identified as a major factor affecting the physical properties of embedded MWNTs. It is of great significance to develop continuum models for MWNTs embedded in an elastic medium. Recently, an elastic double-shell model has been developed to study axially compressed buckling of a DWNT embedded in an elastic medium based on the Donnell equations [33] of linear theory of cylindrical shells [19]. For simplicity, the elastic medium and the nanotube are assumed to possess the same Poisson's ratio and the shear stresses at the tube–medium interface is overlooked.

In this paper, the buckling of a long DWNT embedded in an elastic medium and loaded by a far-field hydrostatic pressure is analyzed using the energy method. The study is on the basis of elastic-shell models. As a DWNT is distinguished from traditional elastic shells by their hollow double-layer structure and the associated van der Waals forces, the effect of van der Waals forces on the buckling is considered. The DWNT is assumed to be thin (the inner radius-to-thickness ratio is larger than five) and the tube is taken to be perfectly bonded to the surrounding medium. In the present model, both normal and shear stresses are included. The difference between the Poisson's ratio of the tube and that of the elastic medium is taken into account. It is assumed that the initial displacements up to the point of buckling are small so that the linear theory holds. An intermediate class of strain-displacement relations as defined by Brush and Almroth [34] is used for shell deformations. In what follows, the inner and outer tubes are assumed to have the same thickness and material constants, and the subscripts 1 and 2 are used to denote the quantities associated with the outer and inner tubes, respectively.

2. van der Waals interaction

The intertube van der Waals forces of a DWNT can be typically modeled by the Lennard–Jones potential [35]. The van der Waals force exerted on any atom on the outer tube can be estimated by adding up all interaction forces between the atom and all atoms on the inner tube. To this end, the latter can be approximated as a flat monolayer because the major contributions come from the neighboring atoms on the inner tube. Hence, the pressure caused by the van der Waals forces at any point on the outer tube can be assumed to be a function of the distance between the inner and outer tubes at that point [35].

As two nested tubes are originally concentric and the initial interlayer spacing is equal or very close to the equilibrium spacing, the initial van der Waals interaction between two tubes of undeformed DWNTs can be overlooked. When the external load is applied, the interlayer spacing changes, and any increase (or decrease) in the interlayer spacing will cause an attractive (or repulsive) van der Waals interaction. For any point on the outer tube, the van der Waals interaction pressure depends linearly on the variation of the interlayer spacing at this point. Thus, the pressure p_1 which is positive inward on the outer tube due to the inner tube can be expressed by [19]

$$p_1 = c(w_1 - w_2), \tag{1}$$

where w_1 and w_2 are the radial displacements of the outer and inner tubes, respectively, which are positive outward. c denotes the van der Waals interaction coefficient, which is defined as

$$c = \left.\frac{\mathrm{d}G(\delta)}{\mathrm{d}\delta}\right|_{\delta=\delta_0}, \tag{2}$$

where $G(\delta)$ is a nonlinear function of the intertube spacing δ, the details of which can be found from the work done by Girifalco and Lad [35]. It is noted that c is a constant which is determined by the slope of the van der Waals law at the initial unbuckled interlayer spacing δ_0 (about 0.34 nm). In accordance with the data provided by Saito et al. [36], the coefficient c can be estimated by

$$c = \frac{320\,\text{erg/cm}^2}{0.16d^2} \quad (d = 0.142\,\text{nm}). \tag{3}$$

Since the van der Waals forces between two tubes are equal and opposite, the value of the pressure p_2 on the inner tube due to the outer tube can be obtained by

$$p_2 = -\frac{a_1}{a_2}p_1, \tag{4}$$

where a_1 and a_2 is the radius of the outer and inner tubes, respectively.

3. Pre-buckling analysis

In this section, the uniform radial displacements of the outer and inner tubes prior to buckling will be obtained. The compressed circular form is taken to be the fundamental equilibrium configuration whose stability is under investigation. Throughout the analysis, the condition of plane strain is assumed, which is shown to be appropriate when the length of the cylinder is more than three times its diameter [37].

3.1. The outer tube and the elastic medium

If the effective pressure acting between the outer tube and the medium is denoted by $\tilde{p}$, the circumferential membrane stress of the outer tube prior to buckling can be obtained by

$$\sigma_{\theta 1} = -\frac{\tilde{p}a_1}{h}, \tag{5}$$

where h is the thickness of the inner and outer tubes.

Assuming the stress–strain behaviour of the shell prior to buckling is linear elastic, it follows from Hooke's law and the condition of plane strain that

$$\varepsilon_{z1} = \frac{1}{E}[\sigma_{z1} - v(\sigma_{r1} + \sigma_{\theta 1})] = 0, \tag{6}$$

where ε_{z1} and σ_{z1} are the axial membrane strain and stress of the outer tube, respectively, and σ_{r1} the radial membrane stress of the outer tube. E and v are Young's modulus and Poisson's ratio of the tube material, respectively. From the above equation, we obtain

$$\sigma_{z1} = v(\sigma_{r1} + \sigma_{\theta 1}). \tag{7}$$

Because there is van der Waals pressure acting on the inner side of the outer tube and the tube is assumed to be thin, the value of σ_{r1} is taken to be equal to this pressure. Thus, it follows from Eq. (1) that

$$\sigma_{r1} = p_{01} = c(w_{01} - w_{02}), \tag{8}$$

where p_{01} is the van der Waals pressure pre-buckling on the outer tube due to the inner tube, and w_{01} and w_{02} are the radial displacements of the outer and inner tubes pre-buckling, respectively. For the circumferential strain, combination of the Hooke's law and Eqs. (5), (7) and (8) gives

$$\varepsilon_{\theta 1} = -\frac{1+v}{E}\left[(1-v)\frac{\tilde{p}a_1}{h} + vc(w_{01} - w_{02})\right]. \tag{9}$$

Noting that the pre-buckling circumferential displacement v_{01} is zero, we have

$$\varepsilon_{\theta 1} = \frac{w_{01}}{a_1}. \tag{10}$$

Consequently, combination of Eqs. (9) and (10) gives

$$w_{01} = R_1\tilde{p} + R_2 w_{02}, \tag{11}$$

with

$$R_1 = \frac{-(1-v^2)a_1^2}{h[E + a_1 cv(1+v)]},$$

$$R_2 = \frac{a_1 cv(1+v)}{E + a_1 cv(1+v)}.$$

Consider now the effective pressure $\tilde{p}$. The radial displacement in the medium is given by [38]

$$u_r = -\frac{1+v_m}{E_m}\left[(p-\tilde{p})\frac{a_1^2}{r} + (1-2v_m)pr\right], \tag{12}$$

where p denotes the far-field hydrostatic pressure, r is the distance from the point to the axis of the tube, and E_m and v_m are Young's modulus and Poisson's ratio of the elastic medium, respectively.

At $r = a_1$, we have $u_r = w_{01}$. Thus the expression of the effective pressure $\tilde{p}$ can be obtained by

$$\tilde{p} = Q_1 p - Q_2 w_{02} \tag{13}$$

with

$$Q_1 = \frac{2(v_m^2 - 1)a_1}{R_1 E_m - (1+v_m)a_1},$$

$$Q_2 = \frac{R_2 E_m}{R_1 E_m - (1+v_m)a_1}.$$

It is noted from Eq. (13) that the effective pressure $\tilde{p}$ reduces to the hydrostatic pressure p when Young's modulus E_m and Poisson's ratio v_m approach 0 and 0.5, respectively, which are the equivalent properties of a fluid.

3.2. The inner tube

The circumferential membrane stress of the inner tube pre-buckling is expressed as

$$\sigma_{\theta 2} = -\frac{p_{02}a_2}{h}, \tag{14}$$

where p_{02} denotes the van der Waals pressure pre-buckling on the inner tube due to the outer tube. From Eqs. (1) and (4), we obtain

$$p_{02} = -\frac{a_1}{a_2}p_{01} = \frac{a_1 c}{a_2}(w_{02} - w_{01}). \tag{15}$$

Combination of the Hooke's law and the condition of plane strain yields

$$\varepsilon_{z2} = \frac{1}{E}[\sigma_{z2} - v(\sigma_{r2} + \sigma_{\theta 2})] = 0, \tag{16}$$

where ε_{z2} and σ_{z2} are the axial membrane strain and stress of the inner tube, respectively, and σ_{r2} the radial membrane stress of the inner tube.

Because the tube is assumed to be thin, the value of σ_{r2} is taken to be zero. Thus, it follows from Eq. (16) that

$$\sigma_{z2} = v\sigma_{\theta 2}. \tag{17}$$

Making use of the Hooke's law for the circumferential strain gives

$$\varepsilon_{\theta 2} = \frac{1}{E}(\sigma_{\theta 2} - v\sigma_{z2}) = \frac{(1-v^2)}{E}\sigma_{\theta 2}. \tag{18}$$

Substitution of Eq. (14) into Eq. (18) gives

$$\varepsilon_{\theta 2} = \frac{(1-v^2)a_1 c}{Eh}(w_{01} - w_{02}). \tag{19}$$

It is noted that the pre-buckling circumferential displacement v_{02} is zero, then

$$\varepsilon_{\theta 2} = \frac{w_{02}}{a_2}. \tag{20}$$

Thus, it follows that

$$w_{02} = Sw_{01} \tag{21}$$

with

$$S = \frac{a_1 a_2 c(1-v^2)}{a_1 a_2 c(1-v^2) + Eh}.$$

Combination of Eqs. (11), (13) and (21) gives

$$w_{01} = \frac{R_1 Q_1}{1 + R_1 Q_2 S - R_2 S}p \tag{22}$$

and

$$w_{02} = \frac{SR_1 Q_1}{1 + R_1 Q_2 S - R_2 S}p. \tag{23}$$

As can be seen, the uniform radial displacements of the outer and inner tubes prior to buckling can be obtained from Eqs. (22) and (23).

4. Buckling analysis

Since the critical load is the load at which a system in equilibrium passes from stable to unstable, it can be determined by finding the lowest load at which the second variation of the total potential energy of the system is nonpositive for at least one possible variation. In the following, the changes in the total potential energy V of the tube-medium structure due to infinitesimal displacements from the above fundamental equilibrium state are considered.

4.1. Energy in the outer tube and the elastic medium

It is known that the strain energies per unit length associated with stretching and bending of the outer tube can be, respectively, expressed as [34]

$$U_{s1} = \frac{Ka_1}{2}\int_0^{2\pi}\left[\frac{v_1' + w_1}{a_1} + \frac{1}{2}\left(\frac{v_1 - w_1'}{a_1}\right)^2\right]^2 \mathrm{d}\theta \tag{24}$$

and

$$U_{b1} = \frac{Da_1}{2}\int_0^{2\pi}\left(\frac{v_1' - w_1''}{a_1^2}\right)^2 \mathrm{d}\theta, \tag{25}$$

where v_1 is the circumferential displacement of the outer tube, $K = Eh/(1-v^2)$, $D = Eh^3/[12(1-v^2)]$, and $v_1' = \mathrm{d}v_1/\mathrm{d}\theta$. From the study of a SWNT, the various values of the effective bending and in-plane stiffness and the corresponding effective Young's modulus and wall thickness have been found [11,39–42]. In this study, the calculation of Yakobson et al. [11] is adopted for the values of these parameters. Using the data of Robertson et al. [43], they found that the effective bending stiffness D is 0.85 eV while the in-plane stiffness $Eh = 360\,\mathrm{J/m^2}$. Furthermore, they also obtained that the thickness of the tube is $h = 0.066$ nm, the corresponding Young's modulus is $E = 5.5$ TPa, and the Poisson ratio $v = 0.19$.

To obtain the second variations in the strain energies associated with stretching and bending of the outer tube, let

$$v_1 = v_{01} + v_{i1}, \qquad w_1 = w_{01} + w_{i1}, \tag{26}$$

where $(v_{01},\ w_{01})$ denotes the above fundamental equilibrium configuration, and the incremental displacement $(v_{i1},\ w_{i1})$ is infinitesimally small. For the circular form, v_{01} and its derivatives and w_{01}' and its derivatives equal zero. Introduction of them into Eqs. (24) and (25) and rearrangement give the equations for the second variations

$$\delta^2 U_{s1} = \frac{K}{a_1}\int_0^{2\pi}\left[(v_{i1}' + w_{i1})^2 + \frac{w_{01}}{a_1}(v_{i1} - w_{i1}')^2\right]\mathrm{d}\theta, \tag{27}$$

$$\delta^2 U_{b1} = \frac{D}{a_1}\int_0^{2\pi}(v_{i1}' - w_{i1}'')^2\,\mathrm{d}\theta. \tag{28}$$

In accordance with Ref. [34], the displacement increments can be assumed as

$$v_{i1} = V_{n1}\sin(n\theta), \tag{29}$$

$$w_{i1} = W_{n1}\cos(n\theta), \tag{30}$$

with $n \geqslant 2$. The cases of $n = 0, 1$ are not considered because these correspond to the dilational and rigid-body motions of the undistorted circular shell.

In order to simplify the analysis, it is assumed that $v_{i1}' + w_{i1} = 0$ everywhere within the outer tube. This assumption is often known as inextensional buckling since the linearized strain $\varepsilon_{\theta 1} = v_1' + w_1$. Thus it follows from

Eqs. (29) and (30) that

$$W_{n1} = -nV_{n1}. \tag{31}$$

The second variations in the strain energies of the outer tube then become

$$\delta^2 U_{s1} = \frac{w_{01}\pi(n^2-1)^2 K V_{n1}^2}{a_1^2}, \tag{32}$$

$$\delta^2 U_{b1} = \frac{\pi n^2 (n^2-1)^2 D V_{n1}^2}{a_1^3}. \tag{33}$$

The potential energy of the pressure p_1 is expressed as [34]

$$\Omega_1 = \int_0^{2\pi} p_1 \left[a_1 w_1 + \frac{1}{2}(v_1^2 - v_1 w_1' + v_1' w_1 + w_1^2) \right] d\theta. \tag{34}$$

Introduction of Eqs. (1) and (26) into Eq. (34) and rearrangement give the equation for the second variation

$$\delta^2 \Omega_1 = \int_0^{2\pi} \Big[c a_1 w_{i1}(w_{i1} - w_{i2}) + \frac{c}{2}(w_{01} - w_{02}) \times (v_{i1}^2 - v_{i1} w_{i1}' + v_{i1}' w_{i1} + w_{i1}^2) \Big] d\theta, \tag{35}$$

where use is made of

$$w_2 = w_{02} + w_{i2}. \tag{36}$$

Substitution of Eqs. (29)–(31) into Eq. (35) gives

$$\delta^2 \Omega_1 = c a_1 \pi n^2 V_{n1}(V_{n1} - V_{n2}) + \frac{c}{2}\pi(1-n^2)(w_{01} - w_{02}) V_{n1}^2. \tag{37}$$

For the energy increase in the surrounding medium caused by the infinitesimally small displacement increment v_{i1} and w_{i1} of the outer tube, it can be obtained by the assumption of conservation of energy. The difference between the work done by the traction forces at the tube–medium interface due to the displacement increments and that done by the elastic medium to the tube through the effective pressure equals the strain energy increase in the medium.

On account of the assumption of perfect bonding between the tube and the medium, at $r = a_1$, the radial and circumferential displacement increments of the medium are

$$u_r^* = w_{i1} = -nV_{n1}\cos(n\theta), \tag{38}$$

$$u_\theta^* = v_{i1} = V_{n1}\sin(n\theta). \tag{39}$$

Ignoring the circumferential displacement at the outer surface of the tube due to rotation of the tube elements, the surface tractions at the tube–medium interface can be expressed as [44]

$$F_n = -\frac{2(n^2-1)(1-v_m)E_m V_{n1}}{(3-4v_m)(1+v_m)a_1}\cos(n\theta), \tag{40}$$

$$F_t = -\frac{(n^2-1)(1-2v_m)E_m V_{n1}}{(3-4v_m)(1+v_m)a_1}\sin(n\theta). \tag{41}$$

Then the work done by these surface tractions to the medium is

$$M_1 = \frac{a_1}{2}\int_0^{2\pi} (F_n u_r^* + F_t u_\theta^*)\, d\theta = \frac{\pi(n^2-1)E_m V_{n1}^2 [(2n-1) - 2v_m(n-1)]}{2(3-4v_m)(1+v_m)}. \tag{42}$$

Simultaneously, through the effective pressure work is being done by the medium to the tube. This work can be obtained by [45]

$$M_2 = \tfrac{1}{2}\pi(n^2-1)\tilde{p} V_{n1}^2. \tag{43}$$

As the first variation $\delta U_m = 0$ from the equilibrium consideration, Fok [44] obtained the second variation of the strain energy of the medium, which is expressed as

$$\delta^2 U_m = 2(M_1 - M_2) = \pi(n^2-1)(B - \tilde{p})V_{n1}^2 \tag{44}$$

with

$$B = \frac{E_m[(2n-1) - 2v_m(n-1)]}{(3-4v_m)(1+v_m)}. \tag{45}$$

4.2. Energy in the inner tube

Under the van der Waals pressure p_2, the strain energies per unit length associated with stretching and bending of the inner tube are

$$U_{s2} = \frac{Ka_2}{2}\int_0^{2\pi} \left[\frac{v_2' + w_2}{a_2} + \frac{1}{2}\left(\frac{v_2 - w_2'}{a_2}\right)^2 \right]^2 d\theta, \tag{46}$$

$$U_{b2} = \frac{Da_2}{2}\int_0^{2\pi} \left(\frac{v_2' - w_2''}{a_2^2} \right)^2 d\theta. \tag{47}$$

To obtain the second variations in the strain energies associated with stretching and bending of the inner tube, let

$$v_2 \to v_{02} + v_{i2}. \tag{48}$$

With $v_{02} = v_{02}' = w_{02}' = w_{02}'' = 0$, substitution of Eqs. (36) and (48) into Eqs. (46) and (47) and rearrangement give the equations for the second variations

$$\delta^2 U_{s2} = \frac{K}{a_2}\int_0^{2\pi} \left[(v_{i2}' + w_{i2})^2 + \frac{w_{02}}{a_2}(v_{i2} - w_{i2}')^2 \right] d\theta, \tag{49}$$

$$\delta^2 U_{b2} = \frac{D}{a_2}\int_0^{2\pi} (v_{i2}' - w_{i2}'')^2\, d\theta. \tag{50}$$

The displacement increments can be assumed as

$$v_{i2} = V_{n2}\sin(n\theta), \tag{51}$$

$$w_{i2} = W_{n2}\cos(n\theta), \tag{52}$$

with $n \geqslant 2$. Assuming $v_{i2}' + w_{i2} = 0$ everywhere within the inner tube, it follows from Eqs. (51) and (52) that

$$W_{n2} = -nV_{n2}. \tag{53}$$

The second variations in the strain energies of the inner tube then become

$$\delta^2 U_{s2} = \frac{w_{02}\pi(n^2-1)^2 K V_{n2}^2}{a_2^2}, \tag{54}$$

$$\delta^2 U_{b2} = \frac{\pi n^2(n^2-1)^2 D V_{n2}^2}{a_2^3}. \tag{55}$$

The potential energy of the pressure p_2 is expressed as

$$\Omega_2 = \int_0^{2\pi} p_2\left[a_2 w_2 + \frac{1}{2}(v_2^2 - v_2 w_2' + v_2' w_2 + w_2^2)\right] d\theta. \tag{56}$$

Thus the second variation is

$$\delta^2\Omega_2 = \int_0^{2\pi}\left[c a_1 w_{i2}(w_{i2} - w_{i1}) + \frac{a_1}{2a_2} c(w_{02} - w_{01}) \times (v_{i2}^2 - v_{i2} w_{i2}' + v_{i2}' w_{i2} + w_{i2}^2)\right] d\theta. \tag{57}$$

Introduction of Eqs. (51)–(53) into the above equation gives

$$\delta^2\Omega_2 = c a_1 \pi n^2 V_{n2}(V_{n2} - V_{n1}) + \frac{a_1}{2a_2} c\pi(1-n^2)(w_{02} - w_{01}) V_{n2}^2. \tag{58}$$

4.3. Determination of the critical load

Since the load p is a far-field hydrostatic pressure, small displacement increments at the interface should not affect the potential energy of the load p, i.e. $\delta^2\Omega = 0$. Then the second variation in the total potential energy is

$$\begin{aligned}\delta^2 V &= \delta^2 U_{s1} + \delta^2 U_{b1} + \delta^2\Omega_1 + \delta^2 U_{s2} + \delta^2 U_{b2} + \delta^2\Omega_2 + \delta^2 U_m \\ &= (\alpha_1 + \beta_1 p) V_{n1}^2 - 2 c a_1 \pi n^2 V_{n1} V_{n2} + (\alpha_2 + \beta_2 p) V_{n2}^2,\end{aligned} \tag{59}$$

with

$$\alpha_1 = \frac{\pi n^2(n^2-1)^2 D}{a_1^3} + \pi(n^2-1)B + c a_1 \pi n^2,$$

$$\beta_1 = \frac{R_1 Q_1 \pi(1-n^2)}{1 + R_1 Q_2 S - R_2 S}\left[\frac{(1-n^2)K}{a_1^2} - \frac{c}{2}(S-1)\right] + \pi(1-n^2) Q_1\left(\frac{1 - R_2 S}{1 + R_1 Q_2 S - R_2 S}\right),$$

$$\alpha_2 = \frac{\pi n^2(n^2-1)^2 D}{a_2^3} + c a_1 \pi n^2,$$

$$\beta_2 = \frac{R_1 Q_1 \pi(1-n^2)}{1 + R_1 Q_2 S - R_2 S}\left[\frac{(1-n^2) S K}{a_2^2} - \frac{a_1}{2a_2} c(1-S)\right].$$

The critical value of p is the smallest load for which the second variation of the total potential energy is not positive definite. Thus we have

$$\delta(\delta^2 V) = 0. \tag{60}$$

As the second variation of the total potential energy given by Eq. (59) is a function of two variables V_{n1} and V_{n2}, we can know that

$$\delta(\delta^2 V) = \frac{\partial(\delta^2 V)}{\partial V_{n1}}\delta V_{n1} + \frac{\partial(\delta^2 V)}{\partial V_{n2}}\delta V_{n2}. \tag{61}$$

Since δV_{n1} and δV_{n2} are arbitrary, the expression in Eq. (61) will vanish if

$$\frac{\partial(\delta^2 V)}{\partial V_{n1}} = 0, \quad \frac{\partial(\delta^2 V)}{\partial V_{n2}} = 0. \tag{62}$$

Carrying out the operations, we obtain

$$(\alpha_1 + \beta_1 p) V_{n1} - c a_1 \pi n^2 V_{n2} = 0, \tag{63a}$$

$$-c a_1 \pi n^2 V_{n1} + (\alpha_2 + \beta_2 p) V_{n2} = 0. \tag{63b}$$

Because the right-hand side of each equation is zero, they are referred to as homogeneous equations. It is obviously that $V_{n1} = V_{n2} = 0$ is one solution to Eq. (63). This is the trivial solution of equilibrium at all loads. The nontrivial solutions of such a problem are obtained by setting the determinant of the governing equations equal to zero. For the case being studied, this means that

$$\begin{vmatrix}\alpha_1 + \beta_1 p & -c a_1 \pi n^2 \\ -c a_1 \pi n^2 & \alpha_2 + \beta_2 p\end{vmatrix} = 0. \tag{64}$$

Expansion of the determinant leads to

$$\beta_1\beta_2 p^2 + (\alpha_1\beta_2 + \alpha_2\beta_1)p + \alpha_1\alpha_2 - c^2 a_1^2 \pi^2 n^4 = 0. \tag{65}$$

This equation is known as the characteristic equation. It determines a relationship between the external pressure p and the buckling mode number n. With each n, the corresponding external pressure p can be identified. The critical pressure for elastic buckling is defined by the lowest pressure with $n \geqslant 2$.

As an example, we assume that $E_m = 2.0\,\text{GPa}$ and $v_m = 0.3$. In addition, let $a_2 = 2.0\,\text{nm}$, then $a_1 = a_2 + \delta_0 = 2.34\,\text{nm}$. As a result, the dependence of the external pressure p on the buckling mode number n is obtained, which is shown in Fig. 1. As can be seen, the external pressure p reaches the minimum at $n = 3$. Thus, the critical pressure p_{cr} is determined by $n = 3$, the value of which is about 0.25 GPa.

5. Discussion

When the van der Waals force is ignored (i.e. $c \to 0$), Eq. (65) reduces to the result obtained by Fok [44]

$$\beta_1 p + \alpha_1 = 0, \tag{66}$$

where β_1 and α_1 become

$$\alpha_1 = \frac{\pi n^2(1-n^2)^2 D}{a_1^3} - \frac{\pi E_m(1-n^2)[(2n-1) - 2v_m(n-1)]}{(3-4v_m)(1+v_m)},$$

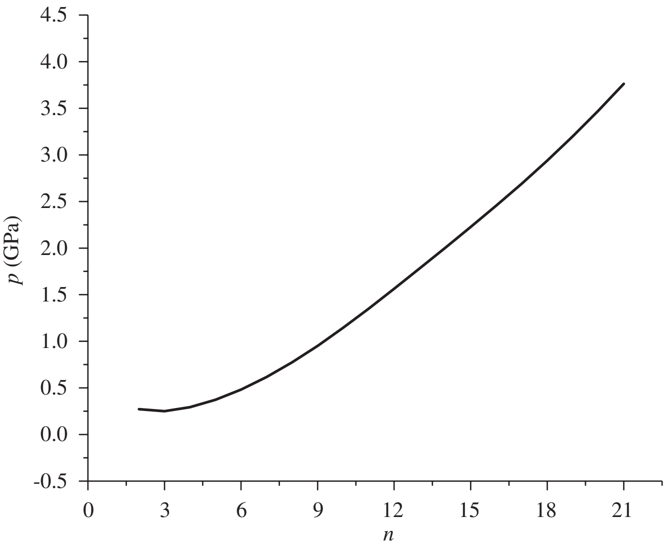

Fig. 1. The dependence of the external pressure p on the buckling mode number n.

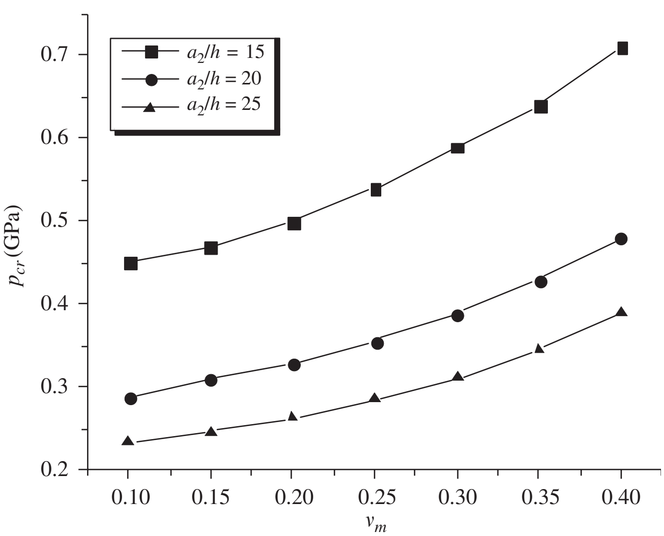

Fig. 2. The effect of Poisson's ratio of the elastic medium on the critical pressure for different inner radius-to-thickness ratios.

$$\beta_1 = \frac{2Eh\pi n^2(1-n^2)(1-v_m^2)}{(1-v^2)a_1E_m + (1+v_m)Eh}.$$

It can be observed that in the absence of van der Waals forces, the elastic buckling of a long DWNT embedded in an elastic medium and under a far-field hydrostatic pressure is independent of the inner tube.

From Eq. (65) and with $E_m = 2.0\,\text{GPa}$, the relationship between the critical pressure p_{cr} and the Poisson's ratio v_m of the elastic medium is obtained for $a_2/h = 15$, 20 and 25, as shown in Fig. 2. It is seen from this figure that at the same inner radius-to-thickness ratio a_2/h, the critical pressure p_{cr} increases with the increment of the Poisson's ratio v_m of the elastic medium, and at the same v_m the critical pressure p_{cr} decreases with increasing the inner radius-to-thickness ratio a_2/h.

On the basis of Eq. (65) and with $v_m = 0.3$, the relationship between the critical pressure p_{cr} and the Young's modulus E_m of the elastic medium is determined for $a_2/h = 15$, 20, and 25, which is indicated in Fig. 3. As can be seen, the critical pressure p_{cr} become larger with increasing the Young's modulus E_m of the elastic medium at the same inner radius-to-thickness ratio a_2/h, and with the same E_m the critical pressure p_{cr} diminishes with the increase of the inner radius-to-thickness ratio a_2/h, which is consistent with the result shown in Fig. 2.

On the other hand, with $E_m = 2.0\,\text{GPa}$ and $v_m = 0.3$, comparison has been made between the values of the critical pressure p_{cr} including the effect of van der Waals force and those ignoring this effect, which is shown in

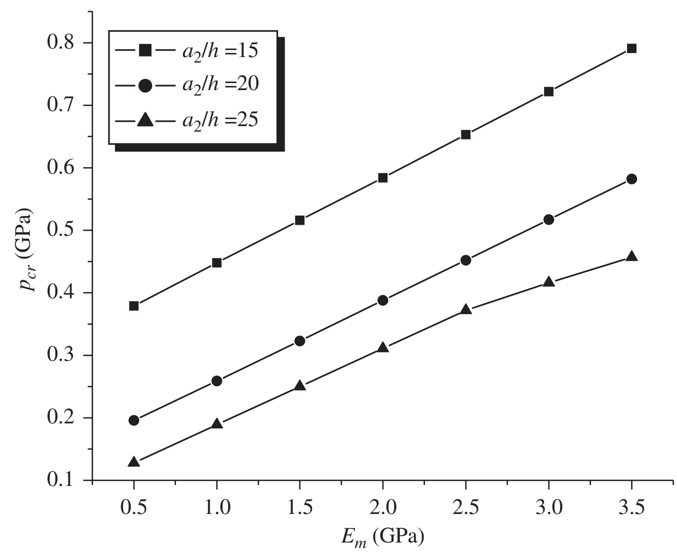

Fig. 3. The effect of Young's modulus of the elastic medium on the critical pressure for different inner radius-to-thickness ratios.

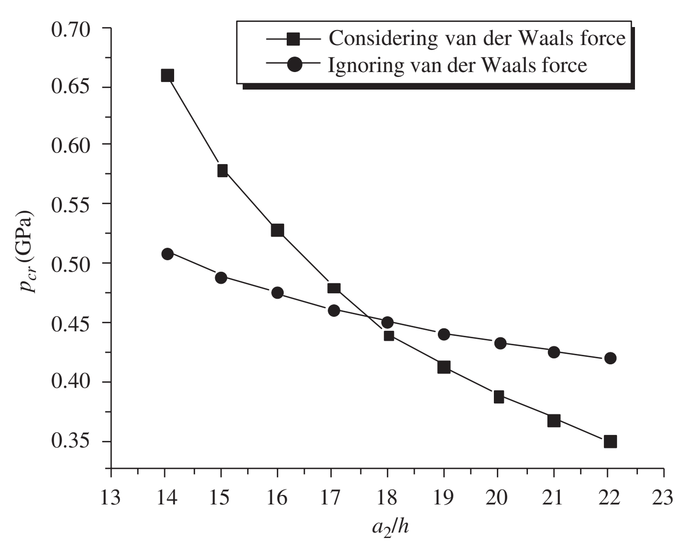

Fig. 4. Comparison of the critical pressure considering the effect of van der Waals force with that ignoring the effect of van der Waals force.

Fig. 4. It is observed that the values of the critical pressure p_{cr} considering the van der Waals forces are larger than those ignoring the van der Waals forces when the values of the inner radius-to-thickness ratio a_2/h are small and are smaller when the values of a_2/h are large. Accordingly, it can be concluded that the influence of the van der Waals force on the critical pressure is dependent on the inner radius-to-thickness ratio.

6. Conclusions

Using the energy method, the elastic buckling of a long DWNT embedded in an elastic medium and loaded by a far-field hydrostatic pressure is analyzed. The DWNT is assumed to be thin and the tube is taken to be perfectly bonded to the surrounding medium. In the present model, both normal and shear stresses at the tube–medium interface are included. The difference between the Poisson's ratio of the tube and that of the elastic medium is taken into account.

An expression is derived relating the external pressure to the buckling mode number, from which the critical pressure can be obtained. Ignoring the van der Waals force, the elastic buckling of a long DWNT embedded in an elastic medium and under a far-field hydrostatic pressure is independent of the inner tube. It is concluded that the critical pressure is dependent on the inner radius-to-thickness ratio, the material parameters of the elastic medium, and the van der Waals force. The influence of the van der Waals force on the critical pressure is dependent on the inner radius-to-thickness ratio.

Acknowledgements

The authors wish to thank the A* STAR (Singapore), SMA (Singapore-MIT Alliance), NSFC (China) under the Grant no. 10372031 for their partial financial support.

References

[1] Ebbesen TW. Carbon nanotubes. Annual Review of Materials Science 1994;24:235–64.
[2] Dresselhaus MS, Dresselhaus G, Eklund PC. Science of fullerenes and carbon nanotubes. San Diego: Academic Press; 1996.
[3] Thomsen C, Reich S, Jantoljak H, Loa I, Syassen K, Burghard M, Duesberg GS, Roth S. Raman spectroscopy on single- and multi-walled nanotubes under high pressure. Applied Physics A 1999;69:309–12.
[4] Maiti A. Mechanical deformation in carbon nanotubes—bent tubes vs tubes pushed by atomically sharp tips. Chemical Physics Letters 2000;331:21–5.
[5] Ru CQ. Degraded axial buckling strain of multiwalled carbon nanotubes due to interlayer slips. Journal of Applied Physics 2001;89:3426–33.
[6] Cohen ML. Nanotubes, nanoscience, and nanotechnology. Material Science Engineering 2001;15:1–11.
[7] Qian D, Wagner GJ, Liu WK, Yu MF, Ruoff RS. Mechanics of carbon nanotubes. Applied Mechanics Review 2002;55:495–533.
[8] Elliott JA, Sandler JKW, Windle AH, Young RJ, Shaffer MSP. Collapse of single-wall carbon nanotubes is diameter dependent. Physical Review Letters 2004;92:095501.
[9] Zhang YQ, Liu GR, Xie XY. Free transverse vibrations of double-walled carbon nanotubes using a theory of nonlocal elasticity. Physical Review B 2005;71:195404.
[10] Zhang YQ, Liu GR, Han X. Transverse vibrations of double-walled carbon nanotubes under compressive axial load. Physics Letters A 2005;340:258–66.
[11] Yakobson BI, Brabec CJ, Bernholc J. Nanomechanics of carbon tubes: instabilities beyond linear range. Physical Review Letters 1996;76:2511–4.
[12] Harris PJF. Carbon nanotubes and related structures. Cambridge: Cambridge University Press; 1999.
[13] Ru CQ. Effective bending stiffness of carbon nanotubes. Physical Review B 2000;62:9973–6.
[14] Saito R, Dresselhaus G, Dresselhaus MS. Physical properties of carbon nanotubes. London: Imperial College Press; 1998.
[15] Kahn CL, Mele EJ. Size, shape, and low energy electronic structure of carbon nanotubes. Physical Review Letters 1997;78:1932–5.
[16] Maiti A, Svizhenko A, Anantram MP. Electronic transport through carbon nanotubes: effects of structural deformation and tube chirality. Physical Review Letters 2002;88:126805.
[17] Lu JP. Elastic properties of carbon nanotubes and nanoropes. Physical Review Letters 1997;79:1297–300.
[18] Wong EW, Sheehan PE, Lieber CM. Nanobeam mechanics: elasticity, strength, and toughness of nanorods and nanotubes. Science 1997;277:1971–5.
[19] Ru CQ. Axially compressed buckling of a doublewalled carbon nanotube embedded in an elastic medium. Journal of the Mechanics and Physics of Solids 2001;49:1265–79.
[20] Wang Q, Hu T, Chen GH, Jiang Q. Bending instability characteristics of double-walled carbon nanotubes. Physical Review B 2005;71: 045403.
[21] Falvo MR, Clary GJ, Taylor RM, Chi V, Brooks GP, Washburn S, Superfine R. Bending and buckling of carbon nanotubes under large strain. Nature 1997;389:582–4.
[22] Lourie O, Cox PM, Wagner HD. Buckling and collapse of embedded carbon nanotubes. Physical Review Letters 1998;81:1638–41.
[23] Yakobson BI, Smalley RE. Fullerence nanotubes: C1000000 and beyond. American Scientist 1997;85:324–37.
[24] Ozaki T, Iwasa Y, Mitani T. Stiffness of single-walled carbon nanotubes under large strain. Physical Review Letters 2000;84: 1712–5.
[25] Wang CY, Ru CQ, Mioduchowski A. Axially compressed buckling of pressured multiwall carbon nanotubes. International Journal of Solids and Structures 2003;40:3893–911.
[26] Zhang YQ, Liu GR, Wang JS. Small-scale effects on buckling of multiwalled carbon nanotubes under axial compression. Physical Review B 2004;70:205430.
[27] Ru CQ. Elastic buckling of singlewalled carbon nanotube ropes under high pressure. Physical Review B 2000;62:10405–8.
[28] Ruoff RS, Tersoff J, Lorents DC, Subramoney S, Chan B. Radial deformation of carbon nanotubes by van der Waals forces. Nature 1993;364:514–6.
[29] Lordi V, Yao N. Radial compression and controlled cutting of carbon nanotubes. Journal of Chemical Physics 1998;109:2509–12.
[30] Ru CQ. Effect of van der Waals forces on axial buckling of a double-walled carbon nanotube. Journal of Applied Physics 2000;87: 7227–31.
[31] Bower C, Rosen R, Jin L, Han J, Zhou OJ. Deformation of carbon nanotubes in nanotube-polymer composites. Applied Physical Letters 1999;74:3317–9.
[32] Qian D, Dickey EC, Andrews R, Rantell T. Load transfer and deformation mechanisms in carbon nanotube-polystyrene composites. Applied Physical Letters 2000;76:2868–70.
[33] Donnell LH. Beams, plates, shells. New York: McGraw-Hill; 1976.

[34] Brush DO, Almroth BO. Buckling of bars, plates and shells. Singapore: McGraw-Hill; 1975.

[35] Girifalco LA, Lad RA. Energy of cohesion, compressibility, and the potential energy functions of the graphite system. Journal of Chemical Physics 1956;25:693–7.

[36] Saito R, Matsuo R, Kimura T, Dresselhaus G, Dresselhaus MS. Anomalous potential barrier of double-wall carbon nanotube. Chemical Physics Letters 2001;348:187–93.

[37] Duns CS, Butterfield R. Flexible buried cylinders, part III: buckling behaviour. International Journal of Rock Mechanics and Mining Sciences 1971;8:613–27.

[38] Moore ID. Elastic buckling of buried flexible tubes—a review of theory and experiment. Journal of Geotechnical Engineering 1989;115:340–58.

[39] Zhou X, Zhou JJ, Ou-Yang ZC. Strain energy and Young's modulus of single-wall carbon nanotubes calculated from electronic energy-band theory. Physical Review B 2000;62:13692–6.

[40] Tu Z, Ou-Yang Z. Single-walled and multiwalled carbon nanotubes viewed as elastic tubes with the effective Young's moduli dependent on layer number. Physical Review B 2002;65:233407.

[41] Kundin KN, Scuseria GE, Yakobson BI. C_2F, BN, and C nanoshell elasticity from ab initio computations. Physical Review B 2001; 64:235406.

[42] Pantano A, Boyce MC, Parks DM. Mechanics of deformation of single and multiwall carbon nanotubes. Journal of the Mechanics and Physics of Solids 2004;52:789–821.

[43] Robertson DH, Brenner DW, Mintmire JW. Energetics of nanoscale graphitic tubules. Physical Review B 1992;45:12592–5.

[44] Fok BO. Analysis of the buckling of long cylindrical shells embedded in an elastic medium using the energy method. Journal of Strain Analysis 2002;37:375–83.

[45] Seide P, Weingarten VI. Buckling of circular rings and long cylinders enclosing an elastic material under uniform external pressure. ARS Journal 1962;32:680–7.